Advances in Science and Technology Research Journal

Advances in Science and Technology Research Journal 2024, 18(2), 333–348
https://doi.org/10.12913/22998624/185255
ISSN 2299-8624, License CC-BY 4.0

Received: 2023.12.13
Accepted: 2024.02.22
Published: 2024.03.15

Computational Fluid Dynamics Studies of a Vertical Axis Wind Turbine with a Variable Swept Area

Idzi Pędzisz[1], Paweł Magryta[1*], Konrad Pietrykowski[1]

[1] Department of Thermodynamics, Fluid Mechanics and Aviation Propulsion Systems, Lublin University of Technology, ul. Nadbystrzycka 36, 20-618 Lublin, Poland

* Corresponding author's e-mail: p.magryta@pollub.pl

ABSTRACT

The article presents the results of the Computational Fluid Dynamics (CFD) research on a vertical axis wind turbine with a variable swept area. The tested turbine has four sets of blades, each of which consists of two moving parts. By changing the angle between these parts, it is possible to change the swept area of the turbine wheel to adjust the characteristics of the turbine to the current wind speed. In the case of strong wind, it is possible to fold blades to protect the rotor against damage. The 3D-CFD model was tested using the ANSYS Fluent software. The four rotors differing in the blade angle were analyzed. The tests were carried out for different wind speeds. The results are presented as pressure and velocity distributions as well as streamlines around the rotor. In addition, the waveforms of the torque acting on a single blade and on the entire rotor are shown. The average rotor torque was also calculated. These findings enabled us to create the characteristics of the power factor for different rotational speeds of the rotor. The results show that the adjustment of the swept area makes the z-turbine have a flexible operating range.

Keywords: vertical axis wind turbine, CFD, ANSYS Fluent, variable geometry.

INTRODUCTION

Wind energy is an increasingly popular and competitive energy source that helps reduce greenhouse gas emissions and sustainably use natural resources. Wind energy can be used to produce electricity and mechanical energy, which makes it a valuable source. It is a form of kinetic energy generated by the movement of air or wind and is created by differences in temperature and atmospheric pressure on Earth. The process of harnessing wind energy in wind turbines involves converting air movement into mechanical energy through the rotation of rotors. The amount of mechanical energy generated by wind turbine depends on several factors such as wind speed, rotor size, the aerodynamic efficiency of blades, and the amount of time the wind blows with a sufficient force [1, 2].

There are many methods to harness wind energy. One way is domestic wind turbines known as micro wind turbines. These are small turbines designed to produce electricity or mechanical energy for individual households, businesses or smaller communities. They are installed on private land and buildings such as houses, farms or small businesses to harness wind energy as a renewable energy source. They enable individuals and communities to use wind energy to generate their own electricity or other types of energy.

One such a type of wind turbines is vertical axis wind turbines (VAWTs) with rotors that rotate around a vertical axis unlike in traditional horizontal axis wind turbines (HAWTs) that have rotors that rotate around a horizontal axis. VAWTs are distinct for is a vertical arrangement of rotors, which resembles a large tower with blades mounted around it. There are many

different designs and configurations of VAWTs, but they tend to be more compact than traditional horizontal-axis turbines [3]. Some characteristics of these turbines are summarized below:

- Compared to HAWTs, VAWTs tend to be smaller and less bulky, so they are more suitable for installation in areas with limited space such as building roofs or urban areas.
- VAWTs are more flexible when it comes to wind direction, as they do not require constant tracking of wind direction as HAWTs do. As a result, they can work efficiently even if wind directions change.
- VAWTs tend to show less efficiency compared to HAWTs in constant wind speeds, especially in strong and stable winds.
- VAWTs can start at lower wind speeds compared to HAWTs, so they are better in areas where winds are less intense.

The last feature is essential because given the average wind speed in Poland at a height of 10 m, which is 3.8 m/s (max. 4.9 m/s), Figure 1, one can easily estimate an average power density of 80 W/m^2 (max. 200 W/m^2) under these very conditions [4].

Most VAWT turbines can begin operation at wind speeds as low as 2-3 meters per second (m/s) or even lower. This is advantageous because they can generate power even at low wind speeds, which can be important in areas with weaker winds. However, VAWT turbines need stronger winds to reach full power. Typically, turbines reach full power in the 10-15 m/s range. At these wind speeds, rotors reach optimum rotation so that they can generate the most electricity.

Vertical axis wind turbines (VAWTs) come in various designs and configurations. They can be classified into different types in terms of their design, i.e aerodynamic features, blade and rotor arrangement or type of axis. Here are some of the most common classifications of VAWTs [6]:

Classification by rotor arrangement:

- single-axis VAWT: rotors rotate around a single vertical axis.
- two-axis VAWT: rotors rotate around two vertical axes, forming an “H”- or “X”-like structure.

Classification by design:

- Darrieus turbine: characterized by “C”- or “S”-shaped blades placed around a central tower.
- Savonius wind turbine: consists of half-circle-shaped blades that rotate around a central axis.

Classification by configuration:

- single-rotor VAWT: consists of a single rotor and is mainly used in small scales such as domestic installations.

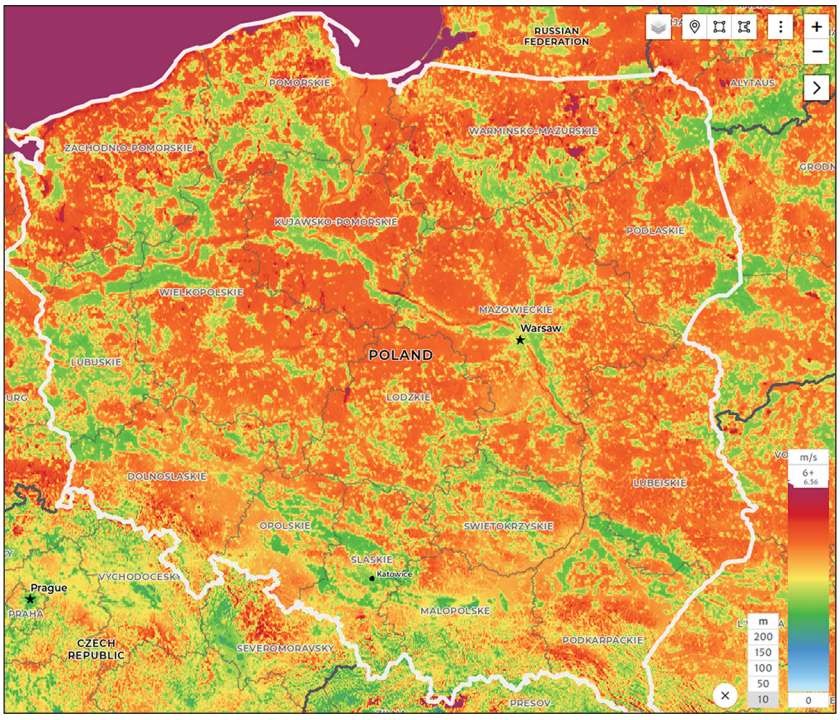

Fig. 1. Map of average wind speeds in Poland at an altitude of 10 m above sea level [5]

- multi-rotor VAWT: consists of multiple rotors that rotate independently, which can increase its efficiency.

Different turbines have different efficiencies. The efficiency of a vertical axis wind turbine (VAWT) depends on many factors, including its design, size, technology and wind conditions it is used. Modern VAWT designs are performing better and gaining in popularity. Average VAWT efficiencies typically range from 20% to 40% [7] but can vary in the type and quality of a particular turbine. This is well illustrated in the graph of the dependence of the torque coefficient C_m and aerodynamic efficiency C_p on the speed ratio TSR.

The torque coefficient is the ratio of the torque generated by the wind turbine T to the dynamic pressure pd, turbine radius R and area A [8]:

$$C_m = \frac{M}{p_d \cdot A \cdot r} = \frac{M}{\frac{1}{2} \cdot A \cdot r \cdot \rho \cdot v^2} \tag{1}$$

where: C_m – torque coefficient of the turbine [-],
M – torque of the turbine [Nm],
p_d – dynamic pressure [Pa],
A – swept area [m^2],
r – blade maximal radius [m],
ρ – air density [kg/m^3],
v – wind speed [m/s].

The aerodynamic efficiency of a vertical axis wind turbine (VAWT) can be expressed by a formula that takes into account the use of kinetic energy of the wind and the generation of mechanical energy by the rotor. The formula for the aerodynamic efficiency of a VAWT turbine is as follows [9]:

$$C_p = \frac{P_t}{P_w} = \frac{P_t}{\frac{1}{2} \cdot \rho \cdot A \cdot v^3} \tag{2}$$

where: C_p – aerodynamic efficiency of the turbine [-],
P_t – power of turbine [W],
P_w – power of the wind [W].

Output mechanical power is the mechanical energy generated by the turbine rotor and depends on rotor speed and torque. Wind kinetic power is the energy contained in the wind flow that passes through the rotor. Wind kinetic power depends on wind speed at the turbine input and its density. It is worth noting that aerodynamic efficiency is one of the factors affecting the overall efficiency of a turbine. The overall efficiency of a turbine, which also takes into account mechanical and electrical losses, will be lower than aerodynamic efficiency.

The second component for evaluating wind turbine efficiency is tip-speed ratio (TSR), is an indicator used in wind turbine efficiency analysis. It determines the relationship between the speed of rotor blade tips and wind speed, which affects the efficiency of the wind turbine. The definition of TSR is the ratio of the peripheral speed of rotor blade tips of a wind turbine to the wind speed at the same point [10]. The formula for TSR can be written as follows:

$$TSR = \frac{\omega \cdot r}{V} \tag{3}$$

where: TSR – tip-speed ratio,
ω – the angular velocity of the tips of the turbine rotor blades,
r – radius of distribution of the tips of the turbine rotor blades,
V – wind speed.

When the TSR value is too small, it means that rotors are too slow compared to wind speed and do not use the full potential of the available kinetic energy of the wind. Conversely, when the TSR value is too high, rotors rotate too fast and there may be losses due to shading effects or overloading of the turbine. The optimal TSR value varies in the type and design of the wind turbine as well as wind speed. In practice, different turbine models and sizes have different ranges of optimal TSR values. Optimizing TSR is a key aspect of wind turbine design to achieve its maximum performance and efficiency in operation.

Most of the wind turbines in use today are shown in Figure 2 by their rotor power coefficient and tip-speed ratio. As can be seen in the chart, the theoretical power coefficient which limits in advance the possible performance of wind turbines is also presented. The presented solutions have some disadvantages due to their design, so each type of the turbines covers only a part of the chart's field. As can be seen, HAWT turbines are located in this statistic in the range of the larger values of the vertical and horizontal axes, while VAWTs are in their range of the fields closer to the smaller values.

The advantages and disadvantages of vertical turbines are summarized [12]. Among the advantages of vertical-axis wind turbines (VAWTs) are:

- flexibility to wind direction: VAWTs are more flexible than traditional horizontal axis wind turbines (HAWTs) in responding to changes

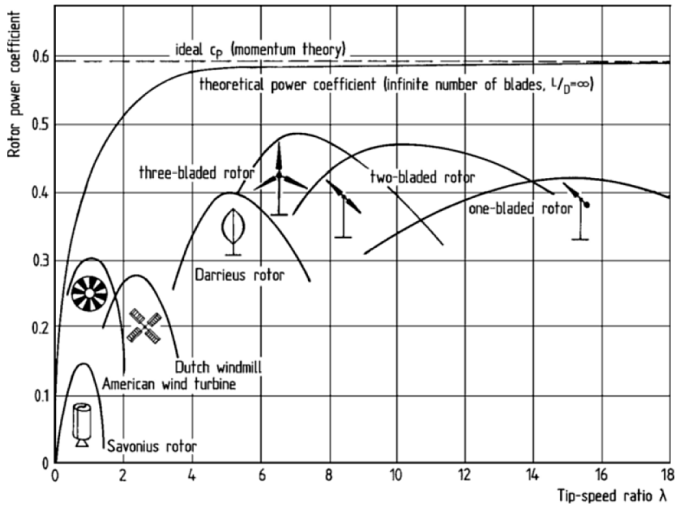

Fig. 2. Rotor power coefficient and Tip-Speed Ratio relationship graph for different wind turbine design solutions [11]

in wind direction. They can operate efficiently even in variable and unpredictable winds.

- small footprint: VAWTs occupy a smaller horizontal footprint than HAWTs, which makes them more suitable for installation in space-constrained areas such as urban rooftops, urban areas or low-wind sites.
- low noise emissions: compared to HAWTs, VAWTs typically generate less noise during operation, which can be advantageous in terms of public acceptance and noise sensitivity around turbines.
- a capability to operate at low wind speeds: VAWTs tend to start operating at lower wind speeds than HAWTs, so they can use winds of lower strength to generate power.

On the other hand, the disadvantages of vertical axis wind turbines (VAWTs) include:

- lower efficiency: VAWTs, compared to HAWTs, tend to have lower efficiency, which means that they convert less energy into electricity. Their aerodynamics are more complicated, which affects overall efficiency.
- complicated design: VAWTs can be more costly to manufacture and maintain and require more advanced technology and materials due to their more complicated blade and rotor design.
- lower prevalence: VAWTs are less common in the market compared to traditional horizontal axis turbines.
- impact on birds and bats: some studies indicate that VAWTs may have a greater impact on birds and bats compared to HAWTs because the spinning rotor is closer to the ground surface these animals often fly.

In addition, each of the turbines must have a power regulation system, and there are many such solutions. Some of the most common methods of power regulation in VAWT turbines [13] are as follows:

- speed control (RPM): In this method, turbine power is controlled by controlling the speed of blades. Controlling the angle of attack or gear angle can affect the turbine speed.
- pitch control (angle of attack control): In this method, the angle of attack of blades is adjusted in response to changing wind conditions. If the wind is too strong, the angle of attack can be reduced to limit the speed and avoid overloading the turbine [14].
- aerodynamic control: In this method, by using different shapes or additional elements on blades, the aerodynamics of the turbine can be adjusted, which affects the power generated [15, 16].
- electrical control: VAWT turbine power control systems can be based on electrical control algorithms that analyze data from wind and load sensors, and then adjust the turbine's operation to achieve optimal performance [17, 18].
- regulation by brake system: In the event of extreme wind conditions or failures, brake systems can be used to stop or reduce turbine speed and minimize the risk of damage.
- regulation by energy storage: In some turbine systems, VAWT can be used to store energy like in batteries or supercapacitors. Power regulation can be achieved by adjusting the amount of energy drawn from or transferred to the storage system [18].

The solution proposed by the authors is based on the obtained patent Pat. 219985 - Rotor with an adjustable position range of blades, in particular for a wind turbine [19] and patent application no. P.441386 - Wind turbine blade angle adjustment mechanism with a variable working surface [20]. The solution assumes the combination of all the advantages of a turbine with a vertical axis, and, characteristically, it has an adjustable working surface. The beneficial effect of the invention is that it is possible to automatically change the angle of wind turbine blades and obtain a variable working surface depending on wind speed, but without stopping the device. This makes the turbine more practical and reduces time required to operate it. The adjustment mechanism also protects the turbine from damage in the event of high-speed winds. In the analyzed solution, it is possible to obtain the maximum possible power of the wind turbine in a wide range of rotor speeds, regardless of wind speed. This is possible because the blade angle can be adjusted and thus the blade surface area is changed. By changing the blade angle, the turbine can adapt to required operating conditions and power. An additional advantage is that the blades can be completely folded in the event of strong winds. This protects the rotor from damage and reduces the requirements for mast strength, which is beneficial in terms of investment costs.

The VAWT consists of four double blades mounted on axes and arranged around the circumference of the hub. The diameter of the rotor is almost constant, and the height of the rotor depends on the blade angle. It can range from 206 mm (for 30°) to 700 mm (for 180°). The rotor design of a turbine set at different blade angles is shown in Figure 3. The design of a single blade is shown in Figure 4, the distance of the blade tip from its axis of rotation is 350 mm, its width is 250 mm, and thickness is 50 mm.

MODEL DESCRIPTION

Geometry of the model

The full model of the vertical axis turbine under study includes elements of mechanisms whose influence on the aerodynamic characteristics is negligible, and for this reason, the turbine geometry was simplified to speed up CFD calculations. Including these details in

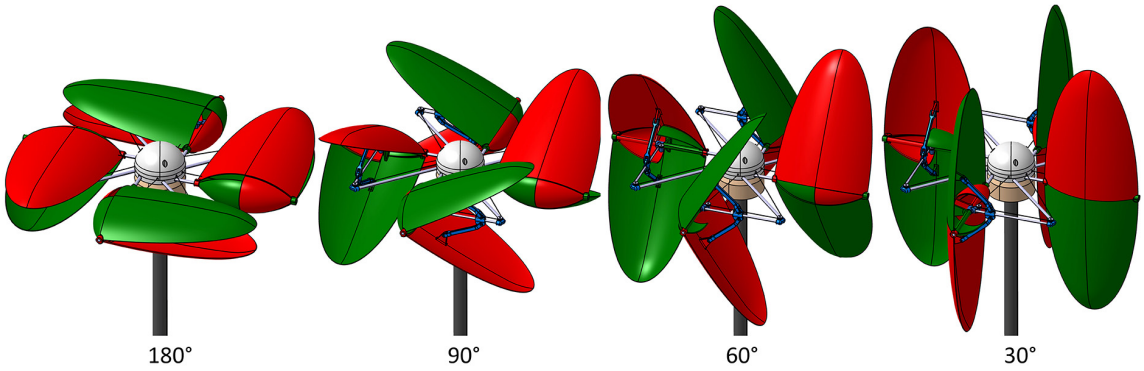

Fig. 3. CAD model view of the wind turbine elaborated by the authors

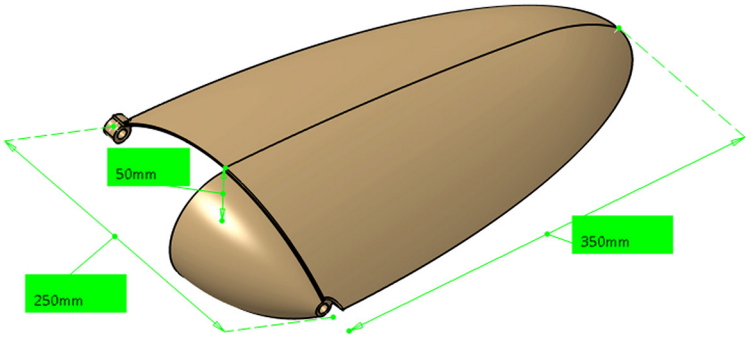

Fig. 4. Turbine rotor blade

the geometry would complicate the computational grid considerably and increase computation time. Due to the fact that the turbine geometry is symmetrical, the calculations were made for one-half of the model. The blade angle controls and the arms the blades are attached with to the turbine stem were removed as shown in Figure 5. The size of the computational domain for this case was: height (half) 1000 mm, length 2700 mm, width 1800 mm. A similar study was conducted by the authors of the publication [21].

The model of the turbine blade geometry was placed in a space corresponding to the dimensions of the real wind tunnel, so it was possible to compare the simulation results obtained with the results of tests conducted in the wind tunnel, which is shown in Figure 6.

- Turbine domain, the cylinder inside which the blade surfaces are tested.
- Ambient domain, the geometry of the wind tunnel interior without the turbine domain.

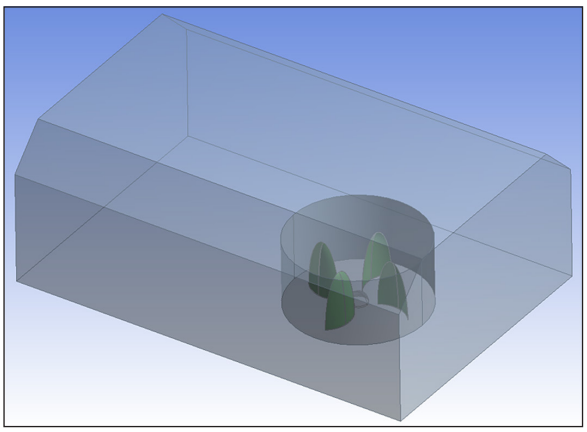

Fig. 5. Simplified model of the turbine in CFD software

Computational mesh

The computational mesh was generated using the ANSYS MESH software. The preferences of the mesh correspond to CFD calculations. It mostly consists of Tetrahedron elements, supplemented by Prism/Wedge elements located in the near-wall layer area. The grid is presented in Figure 7.

The mesh was generated using the following settings given in Table 1. In order to reproduce the effect of the wall layer effect for the surface of the turbine blades and the wind tunnel wall, an inflation parameter was given for these surfaces shown in Figure 8.

The mesh was locally compacted in the turbine blade area using the Body Sizing function (Fig. 9). Then, in order to improve the smoothness of the transition of the nodes of the densified mesh with the mesh present in the rest of the model, the Face Sizing function was applied to the area being separated by the meshes with different parameters.

The surface that is symmetrical was determined at the stage of creating the computational mesh (Fig. 10). The resulting generated mesh contains 2.8 million elements. The average element quality parameter was 0.76196 with a standard deviation of 0.18239.

Table 1. Mesh setting data

Parameter	Value
Relevance centre	Coarse
Smoothing	Medium
Transition	Slow
Min size	1 mm
Max face size	30 mm
Max size	30 mm
Growth rate	1.2

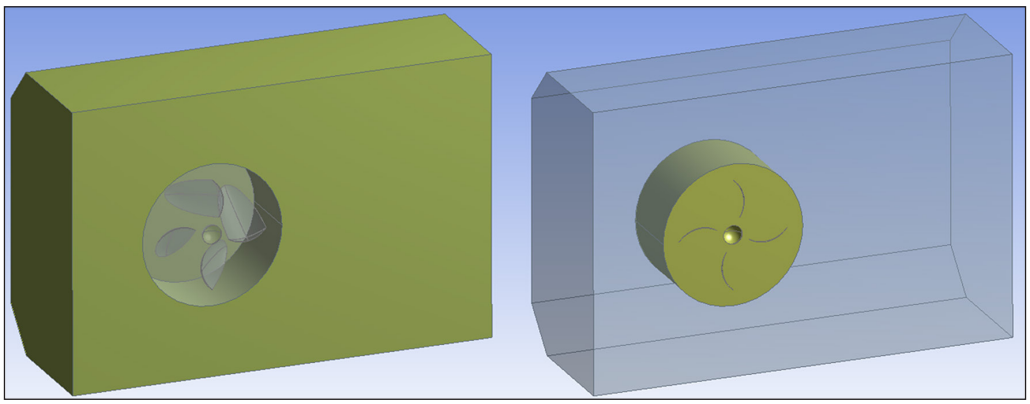

Fig. 6. Ambient domain (left) and turbine domain (right)

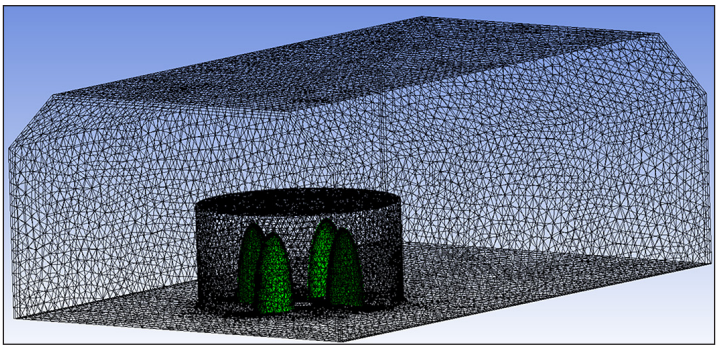

Fig. 7. Image of the computational mesh

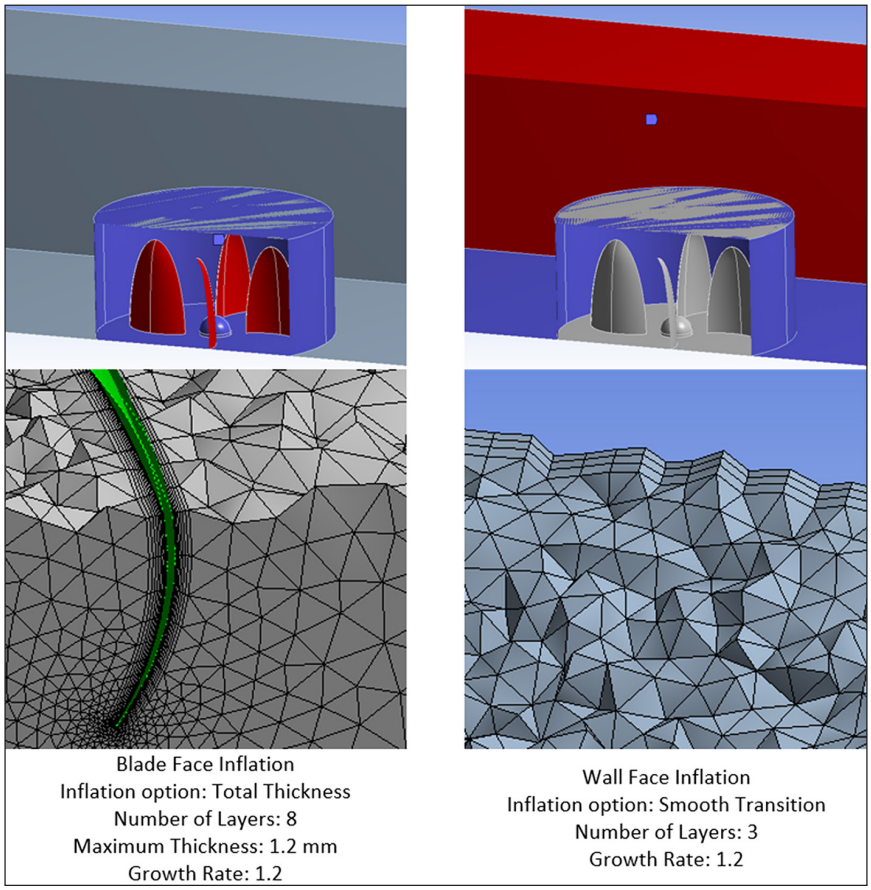

Fig. 8. View of the inflation near the blade surface (left), view of the inflation near the outside walls (right)

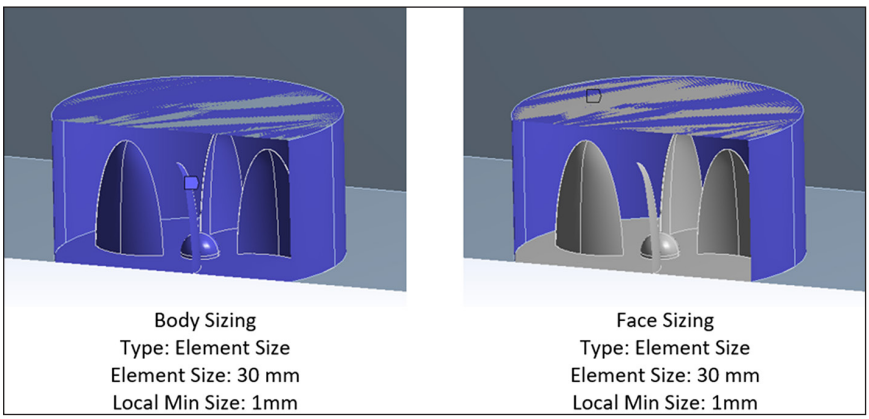

Fig. 9. View of the locations of the body and face sizing regions

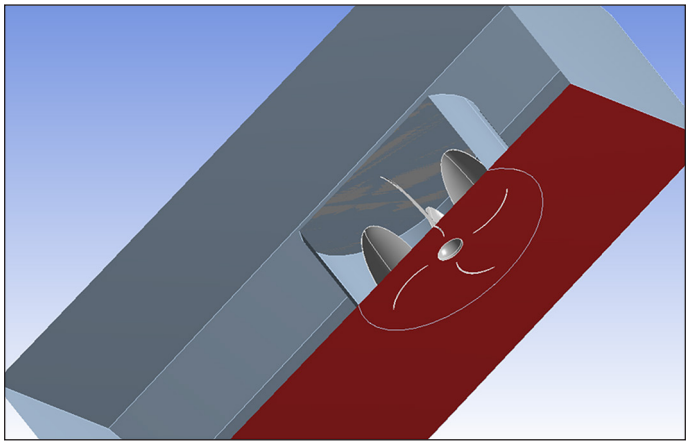

Fig. 10. Area of symmetry

Simulation parameters and course of study

The FLUENT module was used for the calculations, working with the Double Precision setting. The turbulence model used in the study is K-omega in the SST configuration. This model was chosen because of its versatility and popularity. Boundary conditions that were selected (Fig. 11) are:

- Inlet parameters: velocity magnitude: 10 m/s,
- Turbulence specification method: intensity and length scale,
- Turbulent intensity = 0.3%,
- Turbulent length scale = 0.03 m.

Simulation studies were performed only for wind speeds of 10 m/s. It was done so due to the fact that in the future these studies should be compared with the experimental results. At 10 m/s of testing in the wind tunnel, we get better characteristics, i.e. stable operation of the turbine and we can more easily measure the moment.

The motion of the turbine domain the tested blade surfaces are located was defined as a rotary motion with the rotational speed set for each case: 20 rpm, 60 rpm, 100 rpm, 140 rpm, and 180 rpm. The turbine blade surface was defined as a Translational Moving Wall with a speed of 0 m/s, its motion was defined by the parameter Relative to Adjacent Cell Zone.

The simulation was run in a time step that corresponds to two full rotations of the turbine around its axis. The simulation time step was set to correspond to a rotation of 2 degrees. For the turbine model, the simulation needs 360 steps to complete two full rotations.

The simulations were performed for four cases of the turbine blade opening angle: 60˚, 100˚, 140˚, and 180˚ (Fig. 12). Each case was tested for 5 different rotational speeds: 20 rpm, 60 rpm, 100 rpm, 140 rpm, and 180 rpm. A computer equipped with an AMD Ryzen 7 5800H processor with 8 cores and 64 GB of DDR 4 RAM was used for the calculations.

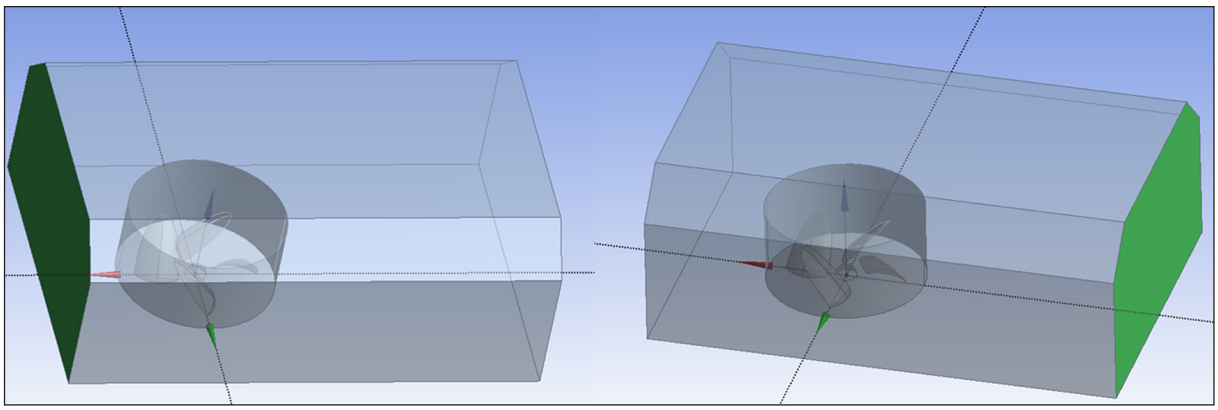

Fig. 11. Velocity inlet location (left) and pressure outlet location (right)

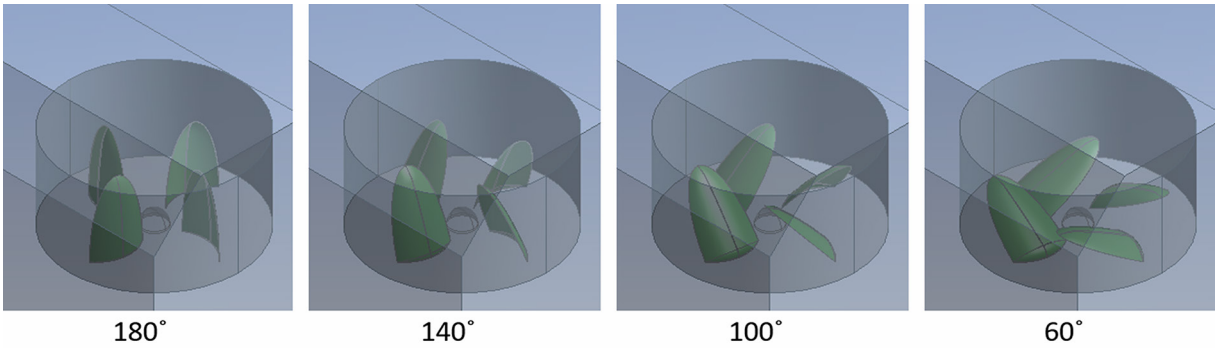

Fig. 12. Four cases of the turbine blade opening angle

RESULTS AND DISCUSSION

Using the ANSYS FLUENT software, the mechanical torque coefficient coarse for each blade surface, pressure and velocity distribution was obtained. Figure 13 shows the method for obtaining the results. The plot shows momentum coefficient values in relation to time. For every case, the simulation time was set to match the time which is needed for the turbine to make two complete rotations. The series named Blade 1-4 shows the values of the momentum coefficient for each of the four blades of the turbine in time. Only the values corresponding to the second rotation are taken into consideration. Preliminary attempts were made to analyze the results at successive rotations of the turbine. The value of the torque at successive revolutions repeated itself after second rotation, so it was decided to present the results for the first two revolutions. The final value is an average taken from the sum of momentum coefficient values for every blade making one rotation.

Figure 14 shows the relationship between the torque generated by the turbine blades to the rotational speed of the turbine at a constant wind speed of 10 m/s for various blade pitch angles. The graph illustrates a non-linear decrease in the torque values concerning the turbine rotational speed. The highest torque, i.e. 4.8 Nm was achieved at the lowest simulated rotational speed of 20 rpm for the model with a blade pitch angle of 100˚. The torque values approach zero before reaching a rotational speed of 180 rpm. For the models with the blade pitch angles of 60 and 100 degrees, the torque value at 180 rpm decreased to the range of +/- 0.1 Nm (approximately 2% of the torque value generated at a rotational speed of

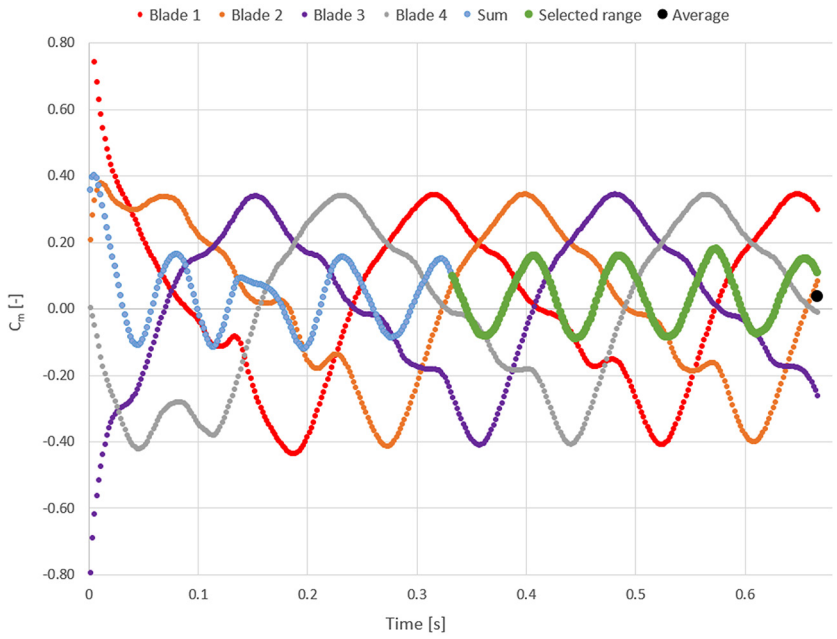

Fig. 13. Methodology of averaging the torque coefficient value from its coarse

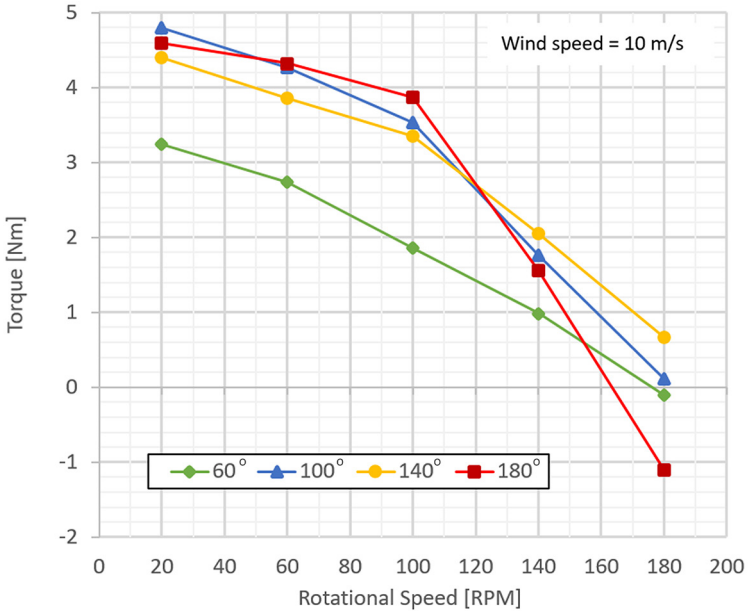

Fig. 14. Relationship between the torque generated by the turbine blades to the rotational speed of the turbine

20 rpm). In the case of a blade pitch angle =140 degrees, the torque value reached the maximum investigated speed of approximately 0.7 Nm (about 15% of the torque generated at a speed of 20 rpm). The chart shows that the values of torque are relatively similar for the cases with the blade pitch angles of 180˚, 140˚ and 100˚, while the values of torque generated by the case with a blade pitch angle of 60˚ are noticeably lower.

Figure 15 shows the relationship between the power generated by the turbine blades to the rotational speed of the turbine at a constant wind speed of 10 m/s for various blade pitch angles. The shape of a graph resembles a non-symmetric parabolic shape with the highest values in the middle and declining further on the both sides. The theoretical value of the power generated by the turbine equals zero if the turbine does not rotate.

All courses depict a non-linear increase in the power values for lower rotational speeds: 20 rpm, 60 rpm, and 100 rpm. The graph shows that for 100 rpm power generated is the highest for all investigated cases. After reaching the highest values for 100 rpm, we can observe a non-linear decline in power generated for the rotational speeds of 140 rpm and 180 rpm.

The highest value of generated power (40.5 W) was achieved for the case with the blade pitch angle of 180˚ at the rotational speed of 100 rpm. The maximum values of power generated for the turbine with a blade pitch angle of 140˚ equals 35 W, a pitch angle of 100˚ equals 37 W and a pitch angle of 60˚ equals 19.5 W.

It is clear in the chart that the values of maximum power are relatively similar for the cases with the blade pitch angles of 180˚, 140˚ and 100˚, while the maximal value of power generated by the case with the blade pitch angle of 60˚ is noticeably lower.

Power values approach zero for the cases with the blade pitch angles of 180˚ and 60˚ before reaching the rotational speed of 180 rpm. For the other angles, the maximum no-load speeds exceed 180 rpm. For models with the blade pitch angles of 60 and 100 degrees, the power value at 180 rpm decreased to the range of +/- 2 W (approximately 1% of the power generated at 100 rpm).

In the case of the blade pitch angle of 140 degrees, the power value reached the maximum investigated speed was approximately 12 W (about 34% of the power generated at 20 rpm).

Figure 16 shows the relationship between the torque coefficient and the rotational speed of the turbine. The waveforms have a similar shape to the torque waveforms. The maximum value of the torque coefficient was reached for the angle of 100 despite the fact that the maximum torque occurs for 180 degrees. This is due to the fact that the torque coefficient relates to the swept area which decreases with the blade angle. The waveform for 60 degrees does not differ from the others, as is the case with the torque waveform. It follows that it is proportional to the swept angle. The torque coefficient waveforms show that the turbine operates most mechanical efficiently for a swept angle of 100 degrees.

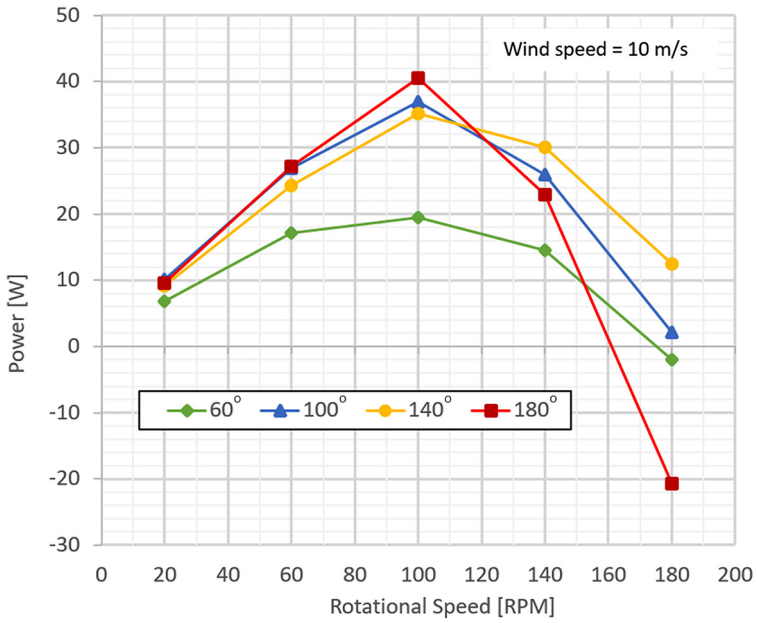

Fig. 15. Relationship between the power generated by the turbine blades to the rotational speed of the turbine

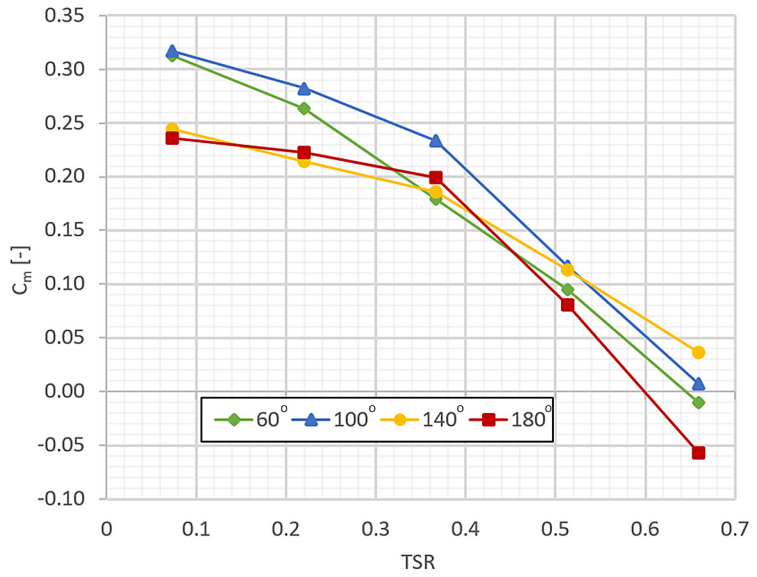

Fig. 16. Relationship between the torque coefficient and the rotational speed of the turbine

Figure 17 shows the relationship between the power coefficient and the rotational speed of the turbine. The shape of the waveforms is similar to the power waveforms. However, the maximum value of the power coefficient was reached for an angle of 100 despite the fact that the maximum power occurs for 180 degrees. This is due to the fact that the power factor relates to the swept area which decreases with the blade angle.

All waveforms have similar values, even the one for 60 degrees does not differ from the rest, which is due to the reduced swept area. The power coefficient tells us about the mechanical efficiency of using the available wind power. The highest rotor mechanical efficiency was obtained for the 100-degree setting angle, as the maximum power factor value of 0.082 was achieved for this angle.

Figure 18 shows the torque generated by a single blade during a single rotation for a blade angle of 100 degrees for different rotational speeds. The graph resembles a sine wave in shape, i.e. there is one minimum and one maximum. Intuitively, it would seem that the highest torque would occur when the blade is positioned perpendicularly to the concave surface against the wind (for a rotation angle of 720), while the lowest torque would occur when the blade is positioned perpendicularly to the convex surface against the wind (for a rotation angle of 540).

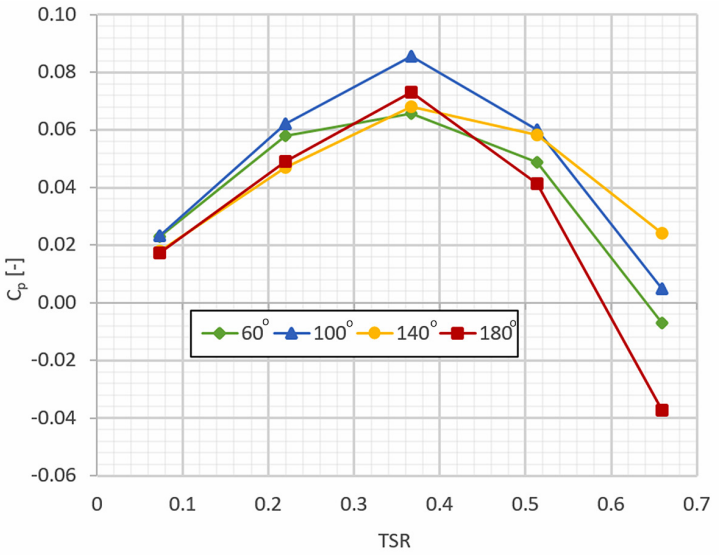

Fig. 17. Relationship between the power coefficient and the rotational speed of the turbine

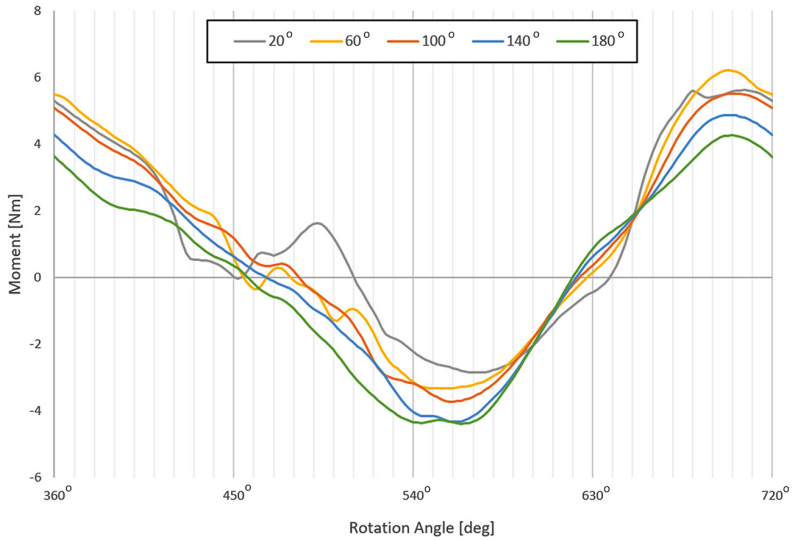

Fig. 18. Torque generated by a single blade during a single totation for the rotation angle of 100 degrees

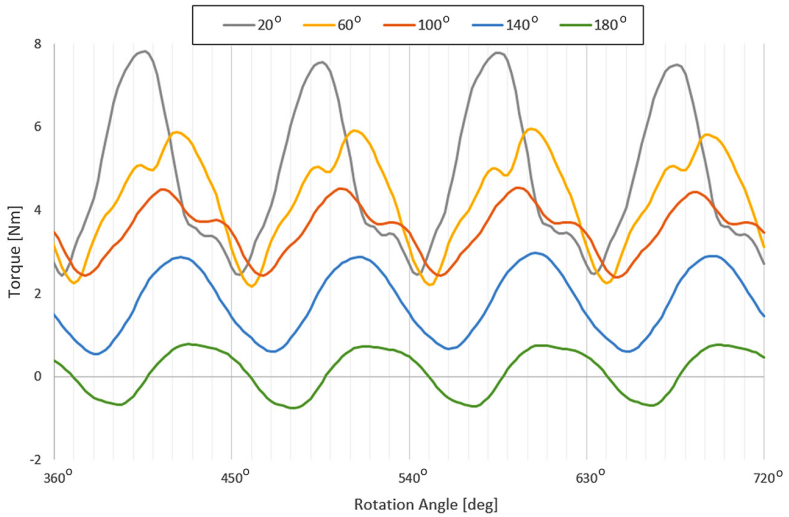

Fig. 19. Torque generated by the turbine rotor in a single rotation for a rotation angle of 100 degrees

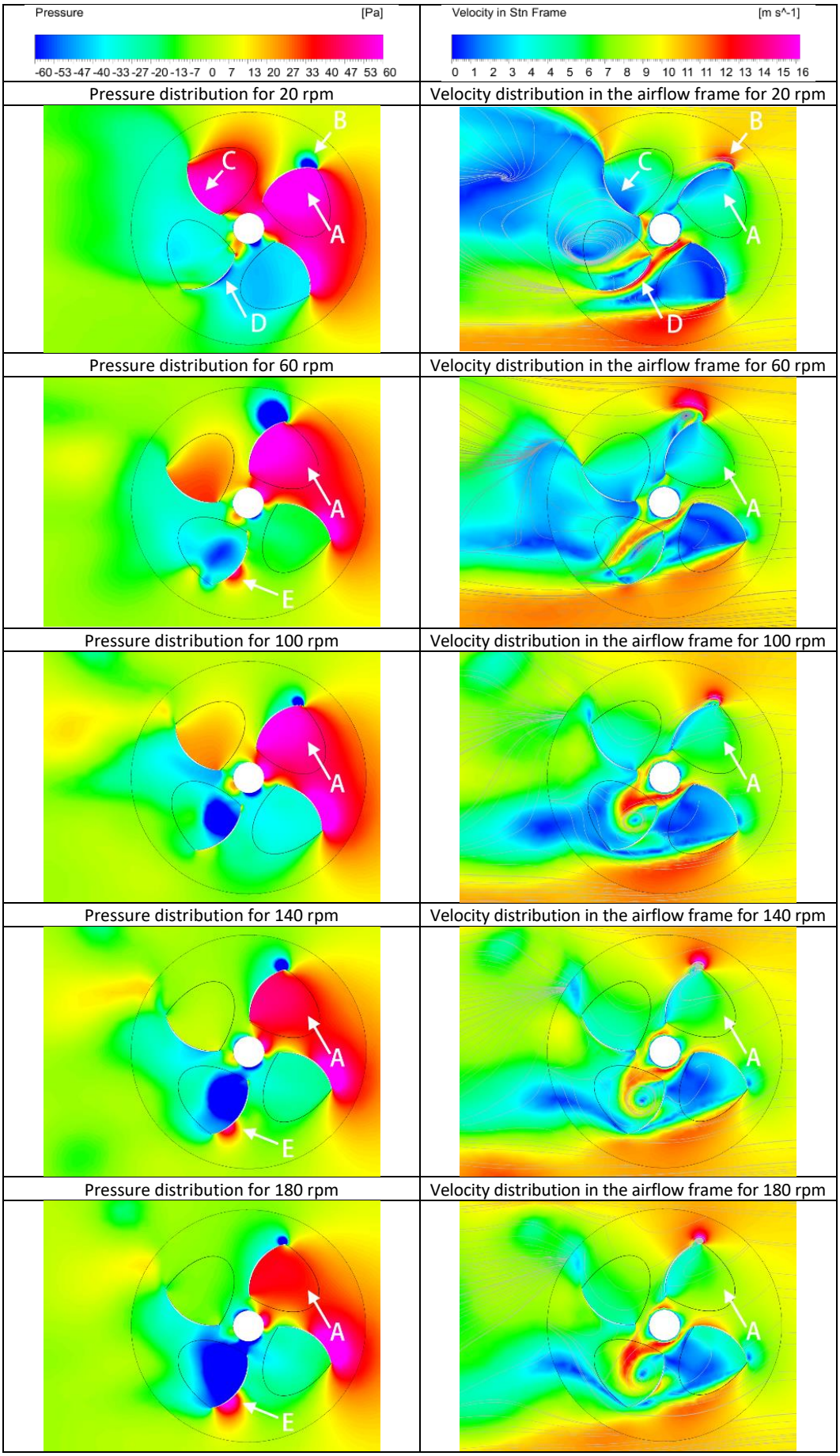

Fig. 20. Distributions of velocity, pressure, and airflow in the section of 0.05 m from the plane of symmetry

In fact, the maximum value of the moment was observed about 20 degrees before reaching a rotation angle of 720, while the minimum value occurs about 20 degrees after reaching a rotation angle of 540. This phenomenon is probably due to aerodynamic interference with the other blades.

At the angle ranging from 420 to 510, when the blade approaches a parallel position (450 degrees) to wind direction at the position furthest from the inlet, disturbances in the torque waveform were observed for all speeds. This is due to the fact that the airflow reaching the blade is disturbed due to the transition between the other turbine blades. The largest disturbance was observed for 20 rpm (rotation angle of 500 degrees). It positively affects the value of the average torque, causing an increase in its average value.

Figure 19 shows the total torque generated by the turbine rotor in a single rotation for the rotation angle of 100 degrees for different rotational speeds. In the chart, we can see a recurring pattern that repeats 4 times in a single rotation. This is due to the number of turbine blades. The torque extremes for different speeds are not reached for the same rotation angle. It was observed that the extreme values occur for similar angles as for a single blade (Fig. 6). As the speed decreases, there is greater irregularity of the waveform (waviness) and greater amplitude of the moment. The torque waveform for 20 rpm is clearly different from the other waveforms. Its maximum value is observed when the turbine blades are set at an angle of 45 degrees into the wind.

Figure 20 shows the distributions of velocity, pressure and waveforms in a section of 0.05 m from the plane of symmetry. For each velocity, the rotation angle for which the maximum torque value was reached was selected. The distributions help explain the factors behind the maximum value. For the case of 20 rpm, we observe a number of phenomena that contribute to the value of the torque generated:

- The largest contribution to torque generation is the high-pressure zone which was formed on the concave part of one of the blades (A) resulting from the decreasing velocity of the airflow coming directly from the intake.
- At the edge of the blade (B), we can observe a high velocity of air flowing around the edge of the blade which then flows along the convex part of the same blade. This causes a region of negative pressure, which increases the moment.
- The air passing the edge of the blade at the point (B) flows onto the concave surface of the next blade decreasing the velocity, resulting in a region of the positive pressure (C).
- A stream of air flowing at high velocity between the blades near the turbine axis (D) is also observed. This stream flows around the convex surface of the blade causing negative pressure which results in a decrease in the resistance of the blade moving against the wind.

The distributions for the other cases (speeds: 60, 100, 140 and 180 rpm) are similar in nature. The most important phenomenon affecting the value of the generated torque is the high-pressure zone.

CONCLUSIONS

In conclusion, the article provides a overview of vertical axis wind turbines (VAWTs) and considerations on their various designs. The key findings can be summarised as follows:

1. The study demonstrates that the power generation of mechanical efficiency of the VAWT is highly sensitive to the blade pitch angle. An optimal blade pitch angle of 100˚ at a rotational speed of 100 rpm generates the highest power output, which emphasizes the key role of precise aerodynamic configurations.
2. The torque and power coefficients exhibit non-linear relationships with rotational speed, which indicates complex aerodynamic interactions between the turbine blades and the incident wind flow. This fact emphasizes the importance of understanding and optimizing the rotational dynamics for efficient power extraction.
3. The analysis of torque distribution in a single rotation reveals the instances of aerodynamic interference between turbine blades, particularly in the range from 420 to 510 degrees.
4. The investigation into torque and power coefficient waveforms demonstrates that the VAWT operates most mechanical efficiently at a swept angle of 100 degrees. This finding suggests that maximizing the swept area while considering aerodynamic factors is critical for achieving optimal mechanical efficiency.
5. The CFD simulations elucidate specific aerodynamic phenomena, including high-pressure zones on the concave blade surface, airflow dynamics at the blade edges, and airflow frame

effects between turbine blades that contribute to torque generation. Understanding these phenomena provides insights into the aerodynamic principles governing turbine performance.

6. The proposed patented solution of adjustable blade angles proves to be an innovative approach for optimizing turbine performance in varying wind conditions. The capability to automatically adapt blade angles without halting turbine operation makes the turbine more practical and resilient to changing environmental conditions.
7. While VAWTs present advantages such as flexibility to wind direction and a smaller footprint, the study acknowledges challenges, including lower mechanical efficiency and complicated design. Addressing these challenges through ongoing research and technological advancements presents opportunities for improving VAWT viability in diverse settings.
8. The study underscores the importance of continued research to refine VAWT designs, optimize control systems, and mitigate potential environmental impacts. Future investigations should focus on scaling up these innovations for real-world applications and assessing their performance in varying wind regimes.
9. Analyzing Figure 15, it can be observe some unpredictable trends in the results obtained. The highest power is obtained for an angle of 180°, then for 100° and then 140°. It has to be noticed that more angle does not mean more power. In addition to the surface area of the blade, the shape of the blade changes, and with it the drag coefficient. At 180°, the highest power was obtained, but the blades are more vertically aligned than at smaller angles and the drag coefficient is higher when moving upwind. Besides, aerodynamic interference between the blades affects the pressure distributions on the individual blades.

The capability of the rotor of the proposed wind turbine to regulate power by changing the blade angle was demonstrated. The maximum power factor was obtained for an angle less than the maximum (180°), which may indicate a suboptimal blade shape. Optimization of the blade shape to increase the power factor for the maximum swept area (180°) can be mentioned as possible future work.

The results obtained should be confirmed by wind tunnel tests. The characteristics of a rotor equipped with an angle adjustment mechanism and other necessary components for operation such as a generator and a mounting mast, will differ from those obtained in simulation studies.

In summary, the scientific insights from this study contribute to the evolving field of vertical axis wind turbines, shed light on intricate aerodynamic interactions and propose innovative solutions to enhance mechanical efficiency and adaptability of turbines.

The efficiency value of presented turbine is small compared to other VAWT turbines, but the turbine has other advantages mentioned in the article. In the future, more research will be conducted to optimize the shape and operation of the turbine, which we hope will translate into increased efficiency.

Acknowledgements

The project/research was financed in the framework of the Lublin University of Technology founds conducting scientific activities FD - discipline fund, funded by the Polish Ministry of Science and Higher Education - Article 365 (2) of July 20, 2018.

REFERENCES

1. Manwell J.F., McGowan J.G., Rogers A.L. Wind Energy Explained - Theory, Design and Application; John Wiley & Sons; 2010.
2. Gipe P. Wind Energy Basics: A Guide to Small and Micro Wind Systems; Chelsea Green Publishing; 2010.
3. Kumar R., Raahemifar K., Fung A.S. A critical review of vertical axis wind turbines for urban applications; Renewable and Sustainable Energy Reviews; 2018; 89; 281-291. https://doi.org/10.1016/j.rser.2018.03.033
4. Pożarska K., Grabowski J. Occurrence of Wind Speed in Selected Places, in North-Eastern Poland in the Aspect of Energy Use; Nauka PrzyrodaTechnologie, 2013; 7:4.
5. Global wind atlas https://globalwindatlas.info/en/area/Poland
6. Eriksson S., Bernhoff H., Leijon M. Evaluation of different turbine concepts for wind power; Renewable and Sustainable Energy Reviews, 2008; 12(5); 1419-1434. https://doi.org/10.1016/j.rser.2006.05.017
7. Luvside, 5 Disadvantages of Vertical Axis Wind Turbine (VAWT), https://www.luvside.de/en/

vawt-disadvantages/

8. Pietrykowski K., Kasianantham N., Ravi D., Gęca M.J., Ramakrishnan P., Wendeker M. Sustainable energy development technique of vertical axis wind turbine with variable swept area – An experimental investigation, Applied Energy; 2023, 329 (120262). https://doi.org/10.1016/j.apenergy.2022.120262
9. Brusca S., Lanzafame R., Messina M. Design of a vertical-axis wind turbine: how the aspect ratio affects the turbine's performance; International Journal of Energy and Environmental Engineering; 2014; 5; 333–340. https://doi.org/10.1007/s40095-014-0129-x
10. Posa A. Influence of Tip Speed Ratio on wake features of a Vertical Axis Wind Turbine; Journal of Wind Engineering and Industrial Aerodynamics; 2020; 197; 104076. https://doi.org/10.1016/j.jweia.2019.104076
11. Castillo O.C., Andrade V.R., Rivas J.J.R., González R.O. Comparison of power coefficients in wind turbines considering the tip speed ratio and blade pitch angle. Energies; 2023, 16(6), 2774. https://doi.org/10.3390/en16062774
12. Saad M.M.M., Asmuin N. Comparison of horizontal axis wind turbines and vertical axis wind turbines. IOSR Journal of Engineering; 2014; 04 (08); 27-30. https://doi.org/10.9790/3021-04822730
13. Samsonov V., Baklushin P. Comparison of different ways for VAWT aerodynamic control. Journal of Wind Engineering and Industrial Aerodynamics; 1992; 39 (1–3); 427-433, https://doi.org/10.1016/0167-6105(92)90566-S
14. Abdalrahman G., Melek W., Lien F-S. Pitch angle control for a small-scale Darrieus vertical axis wind, turbine with straight blades (H-Type VAWT). Renewable Energy; 2017; 114 (B), 1353-1362. https://doi.org/10.1016/j.renene.2017.07.068
15. Hwang I.S., Min S.Y., Jeong I.O., Lee Y.H., Kim S.J. Efficiency improvement of a new vertical axis wind turbine by individual active control of blade motion. Smart Structures and Integrated Systems; 2006; 6173. https://doi.org/10.1117/12.658935
16. Czyż Z., Kamiński Z. The characteristics of the operating parameters of the vertical axis wind turbine for the selected wind speed. Adv. Sci. Technol. Res. J.; 2017; 11(1); 58–65, https://doi.org/10.12913/22998624/68469
17. Gryniewicz-Jaworska M. Application of heuristic optimization for the selection of parameters of the generation system and reactive power consumption of wind farms; Adv. Sci. Technol. Res. J.; 2020; 14(3):9–14. https://doi.org/10.12913/22998624/120929
18. Czyż Z., Karpiński P., Klepka T., Szkoda Z. Design and simulation of small-scale horizontal-axis wind turbine with diffuser effect. MATEC Web Conf.; 2019; 252. https://doi.org/10.1051/matecconf/201925204005
19. Patent no. Pat. 219985 - Rotor with an adjustable position range of blades, in particular for a wind turbine
20. Patent application no. P.441386 - Wind turbine blade angle adjustment mechanism with a variable working surface.
21. Czyż Z., Kamiński Z., Wendeker M. Wind turbine operation parameter characteristics at a given wind speed. Adv. Sci. Technol. Res. J. 2014; 8(22):75-82. https://doi.org/10.12913/22998624.1105178